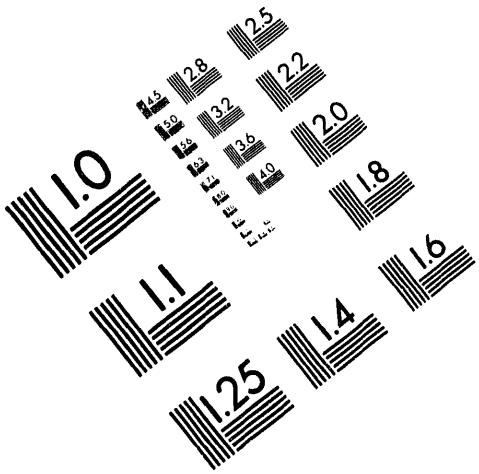

Association for Information and Image Management
1100 Wayne Avenue, Suite 1100
Silver Spring, Maryland 20910
301/587-8202

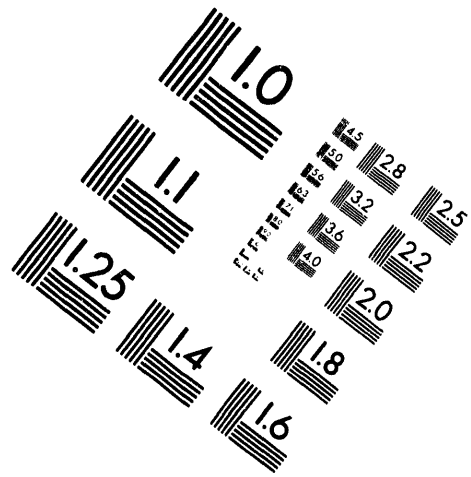

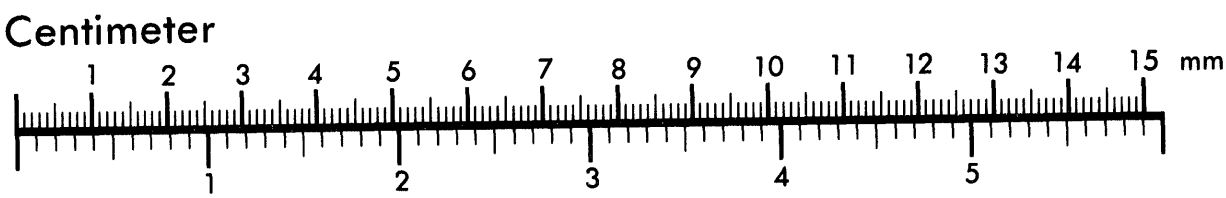

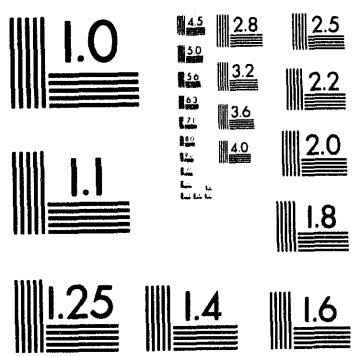

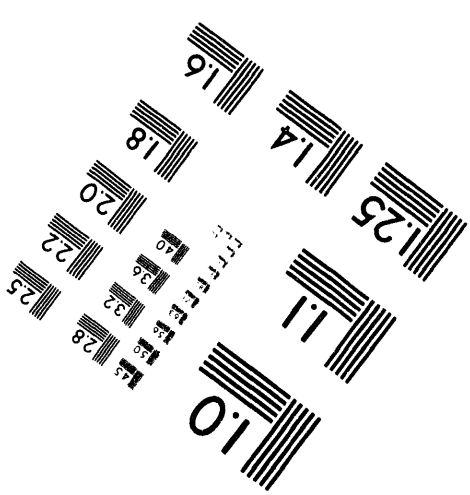

MANUFACTURED TO AIIM STANDARDS
BY APPLIED IMAGE, INC.

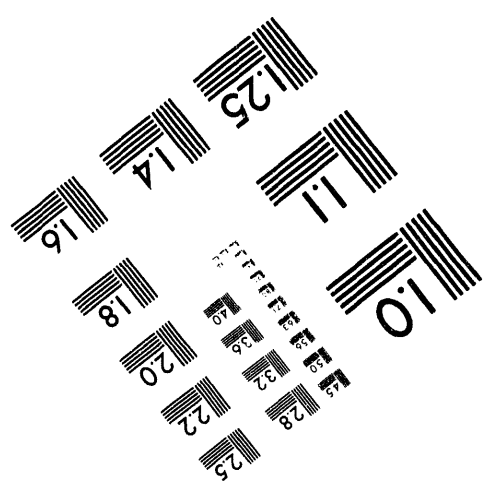

1 of 1

Conf-940524--3

DEVELOPMENT OF SELF-ABSORPTION COEFFICIENTS FOR THE DETERMINATION OF GAMMA-EMITTING RADIONUCLIDES IN ENVIRONMENTAL AND MIXED WASTE SAMPLES*

W. Elane Streets
Analytical Chemistry Laboratory
Chemical Technology Division
Argonne National Laboratory
Argonne, IL 60439

ABSTRACT

As the need for rapid and more accurate determinations of gamma-emitting radionuclides in environmental and mixed waste samples grows, there is continued interest in the development of theoretical tools to eliminate the need for some laboratory analyses and to enhance the quality of information from necessary analyses. In gamma spectrometry the use of theoretical self-absorption coefficients (SACs) can eliminate the need to determine the SAC empirically by counting a known source through each sample. This empirical approach requires extra counting time and introduces another source of counting error, which must be included in the calculation of results. The empirical determination of SACs is routinely used when the nuclides of interest are specified; theoretical determination of the SAC can enhance the information for the analysis of true unknowns, where there may be no prior knowledge about radionuclides present in a sample. Determination of an exact SAC does require knowledge about the total composition of a sample. In support of the Department of Energy's (DOE) Environmental Survey Program, the Analytical Chemistry Laboratory (ACL) at Argonne National Laboratory developed theoretical self-absorption models to estimate SACs for the determination of non-specified radionuclides in samples of unknown, widely-varying, compositions. Subsequently, another SAC model, in a different counting geometry and for specified nuclides, was developed for another application. These two models are now used routinely for the determination of gamma-emitting radionuclides in a wide variety of environmental and mixed waste samples.

*Work supported by the U.S. Department of Energy under Contract W-31-109-Eng-38.

As the need for rapid and more accurate determinations of gamma-emitting radionuclides in environmental and mixed waste samples grows, so does interest in the development of theoretical tools to eliminate the need for some laboratory analyses and to enhance the quality of information from necessary analyses. In gamma spectrometry, the use of theoretical self-absorption coefficients (SACs) can eliminate the need to determine the SAC empirically by counting a known source through each sample. This empirical approach requires extra counting time and introduces another source of counting error which must be included in the calculation of results. The empirical determination of SACs is routinely used when the nuclides of interest are specified; theoretical determination of the SAC can enhance the information for the analysis of true unknowns, where there may be no prior knowledge about radionuclides present in a sample. Determination of an exact SAC does require knowledge about the total composition of a sample.

In support of the Department of Energy's (DOE) Environmental Survey Program, the Analytical Chemistry Laboratory (ACL) at Argonne National Laboratory (ANL) developed theoretical models to estimate SACs for the determination of non-specified radionuclides in samples of unknown, widely varying, compositions. Subsequently, another SAC model was developed for another application employing a different counting geometry and for specified nuclides. These two models are now used routinely for the determination of gamma-emitting radionuclides in a wide variety of environmental and mixed waste samples.

Gamma-emitting radionuclides in environmental samples are typically determined using equipment adapted and dedicated to that purpose, such as germanium detectors fitted with Marinelli beakers. As a multidisciplinary service laboratory, the ANL/ACL could not afford to

dedicate equipment to periodic low-level analysis requests; therefore, it had to adapt its existing multi-use equipment to determine gamma activities in environmental samples. Germanium detectors of both vertical and horizontal configurations were calibrated for the analysis of this type sample. The detectors were calibrated for close-geometry efficiency by counting standards in a set configuration (a height of 6.4 cm in a 4-oz. wide-mouthed Nalgene bottle) immediately adjacent to the cryostat face. This configuration was chosen so that the standards would be symmetrical to the centers of both the horizontal and vertical detectors, as shown in Fig. 1.

Radioactive calibration standards (two solids and two liquids) were prepared and counted in a fixed geometry adjacent to the detector, to determine the close-geometry efficiency curve for each detector used for determination of low-level radionuclides.

The two solid standards were prepared by adding a known amount of Standard Reference Materials NBL (New Brunswick Laboratory, Argonne, IL) No. 6-A (Pitchblende) and NBL No. 7-A (Monazite Sand) to a blanked soil and mixing. Homogeneity of the standards was checked by counting each standard at each quadrant (on a horizontal detector). The final mixtures showed less than 1% deviation between the high and low quadrant counts.

The two liquid secondary standards were prepared from stock solutions of ^{137}Cs, ^{131}I, and ^{110m}Ag, which had been characterized as point sources using several detector efficiency curves. These efficiencies were determined using point source standards from the National Institute of Standards Technology (NIST) and the International Atomic Energy Agency (IAEA).

All standards had activity levels that allowed less than 1% counting statistics to be obtained on the major peaks (i.e., those with stronger branching ratios) within two hours.

Analysis of the resulting data yielded smooth efficiency curves for each of the six detectors, as typified by Fig. 2. Although the compositions of the standards varied from solid to liquid, the densities were all $\simeq 1.0$ g/cm^3.

Ideally, environmental samples would consist of filtered waters and dried, ground, and homogenized soils. These types of preparation yield samples similar in composition to the standards used to calibrate the detector systems. These samples are then prepared in the same fixed geometry as the standards and measured relative to the efficiency curve.

However, actual field samples submitted for analysis can vary significantly in matrix composition, including soils, sludges, vegetation, waters, and liquid organics. In addition, some programs require measurements to be made on samples as received from the field (i.e, no drying, grinding, or homogenization), and sample densities can vary significantly from the density of the calibration standards (1 g/cm^3). Because of this variation in sample matrix, some attempt at correcting for gamma-ray self-absorption became necessary.

Rigorous calculation of SACs is not feasible since this would require complete characterization of a wide variety of samples to determine the true mass absorption coefficient. The empirical determination of SACs by counting known gamma-emitting sources through the sample can be used when the nuclides of interest are specified; however, this empirical approach requires extra counting time and introduces another source of counting error, which must be included in the calculation of results. Theoretical determination of the SAC can enhance the information for the analysis of true unknowns, where there may be no prior knowledge about radionuclides and matrix composition present in a sample, and can also eliminate the need for an extra sample count. This paper presents a theoretical approach based

on sample density, since this parameter is simple to determine when sample weights are obtained in the specified geometry.

The model used depends on the detector configuration. For vertical detectors, a simple model has been developed using the equation for self-absorption in a linear source [1],

$$\frac{I}{I_0} \simeq \frac{1-e^{(-\mu_m \rho x)}}{\mu_m \rho x}$$

where μ_m = mass absorption coefficient,

ρ = sample density, g/cm^3,

x = sample height in bottle, 6.4 cm

For horizontal detectors, the model uses the equation for self-absorption in a cylinder [1],

$$\frac{I}{I_0} \simeq e^{-(8/3\Pi)\mu_m \rho r}$$

where μ_m and ρ are as defined above, and r is the radius of the bottle used, 2.5 cm.

These simple models assume that the radioactivity is uniformly distributed in the sources and that one has a point detector. Also, absorption due to the polypropylene bottle is not considered since it is assumed to be a constant for all the standards and samples.

Using available data for experimental mass absorption coefficients for pure elements [2], self-absorption factors were calculated for energies of 200, 400, 600, 800, 1000, 1500, and 2000 keV, which cover the range of gamma-ray energies determined in our analyses. The following elements were chosen to span the range of densities expected in the samples [3].

Element	Density, ρ = g/cm^3 [3]
Li	0.534
K	0.86
Na	0.97
Ca	1.54
Mg	1.74
S	2.07
Si	2.33
Al	2.702

These SACs were calculated for both models, but in this paper, only the results for the horizontal detector geometry are shown; results for the vertical geometry detectors are parallel, and show the same trends. Table 1 shows the calculated values, and Figure 3 presents plots of these data for the horizontal detector geometry.

Since the efficiency curve represents an inherent correction for ρ = 1 g/cm^3, the SACs could not be used directly to correct the raw data, but first had to be normalized to the theoretical correction at ρ = 1 g/cm^3. Because sodium was the element with ρ closest to 1 g/cm^3, it was chosen as the normalization point; and the correction factor at a given energy and density becomes

$$\text{Correction Factor } (E, \rho_Q) = \frac{\text{SAC, Na } (\rho = 0.97)}{\text{SAC, Element Q } (\rho = \rho_Q)}$$

The correction factors for the horizontal model are given in Table 2.

Graphs of these calculated correction factors versus the corresponding energy were then constructed for the seven densities listed [Fig. 4] to allow estimation of correction factors at densities and energies other than the ones specified in the table..

In order to incorporate these correction factors into a computer program to automatically generate the correction factor for a given gamma energy and sample density, these curves were then fitted by the method of least squares to various equations (Table 3). For both geometries, the power curve gave the best fit:

$$\text{Correction Factor } (E, \rho_Q) = A\,(E, \text{keV})^{B}$$

with coefficients A and B varying with the density and the geometric model used.

The equation coefficients (A and B) were then plotted versus the density [Figs. 5 & 6]. Regression analysis yielded best fits of A to an exponential equation ($A = Ce^{D\rho}$) and B to a linear equation ($B = E + F\,\rho$), where C, D, E, and F represent constants for each detector geometry. With these equations the coefficients A and B can be derived for use in the power curves used for the calculation of the correction factors. Here ρ represents the experimental sample density, in our case the sample weight in grams divided by the volume of our fixed-geometry bottle, 120 mL. Using these equations, a correction factor can be calculated for any nuclide energy (200-2000 keV) for samples of density $0.534 < \rho < 2.702$ g/cm^3.

The computer programs incorporating these models and using these estimated coefficients have been used to derive Correction Factors for the densities of the pure elements used to construct the models. These have been compared with the experimental Correction Factors for the pure elements in Table 4. The worst fit of a calculated versus experimental Correction factor at a given density/energy combination is -4.6% , which provides an adequate

estimate for these type samples.

Analytical results for a wide range of gamma-ray energies and sample densities have been demonstrated to be satisfactory over the calibrated range of energies. For these analyses, NIST environmental-level soil standards (SRM 4353 and SRM 4350B) have been used as laboratory control samples for this procedure (both at densities of ~0.8 g/cm^3) . In addition, these models have been used to determine low-level gamma-emitting nuclides in the Soil, Vegetation, and Water matrices provided by the Environmental Measurements Laboratory Quality Assessment Program (EML QAP); the varying densities of these matrices provide another test for these models. The density of the water sample is ~ 1 g/cm^3; however the soil density has varied historically, during our period of participation, from ~ 1 to 1.6 g/cm^3, and the vegetation density from ~.65 to .85 g/cm^3. The historical data for the determination of Cs-137 in these three matrices are shown in Figs. 7-9. These data represent results from both geometrical models. In general, there is very good agreement between the ANL results, the EML results, and the mean results for all three matrices, with no obvious bias.

The use of these theoretical SACs has been shown to be adequate for correcting for self-absorption of gamma radiation in environmental samples. This theoretical approach can be applied to a broad spectrum of samples whose matrix and radionuclide composition is unknown. It also allows for faster analysis by elimination of the second sample count required by the empirical approach. The final curve-fitting to allow estimation of the necessary coefficients provides a mathematical model which can be easily incorporated into computer programs for automatic data analysis. Thus, the theoretical approach has both economic and technical merit.

References

[1] R. D. Evans and R. O. Evans, Rev. Mod. Phy., 20:305 (1948).

[2] Nuclear Data Tables, Section A, Vol. 7, No. 6, June 1970. "Photon Cross Sections from 1 keV to 100 MeV for Elements Z=1 to Z=100," Ellery Storm and Harvey I. Israel.

[3] CRC Handbook of Chemistry and Physics, 68th Edition, CRC Press Inc., 1987-88.

Figures

1. Experimental Counting Configurations
2. Close-Geometry Efficiency Curve
3. Self-Absorption Coefficients, Horizontal Detectors
4. Correction Factors, Horizontal Detectors
5. Coefficients A, Horizontal Detectors
6. Coefficients B, Horizontal Detectors
7. Cs 137 in Soil, EML QAP
8. Cs 137 in Vegetation, EML QAP
9. Cs 137 in Water, EML QAP

Figure 1
Experimental Counting Configurations

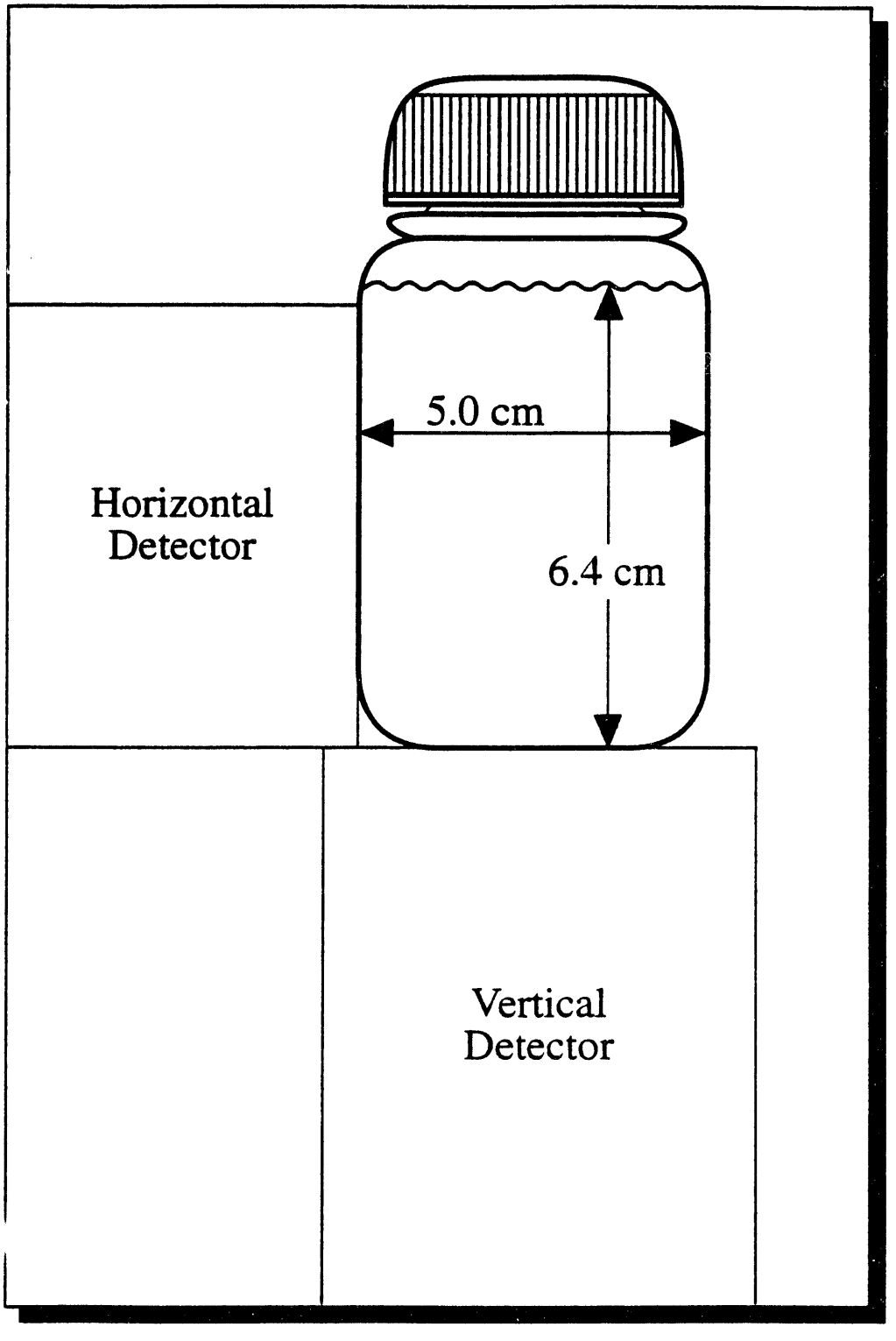

Figure 2

Close-Geometry Efficiency Curve

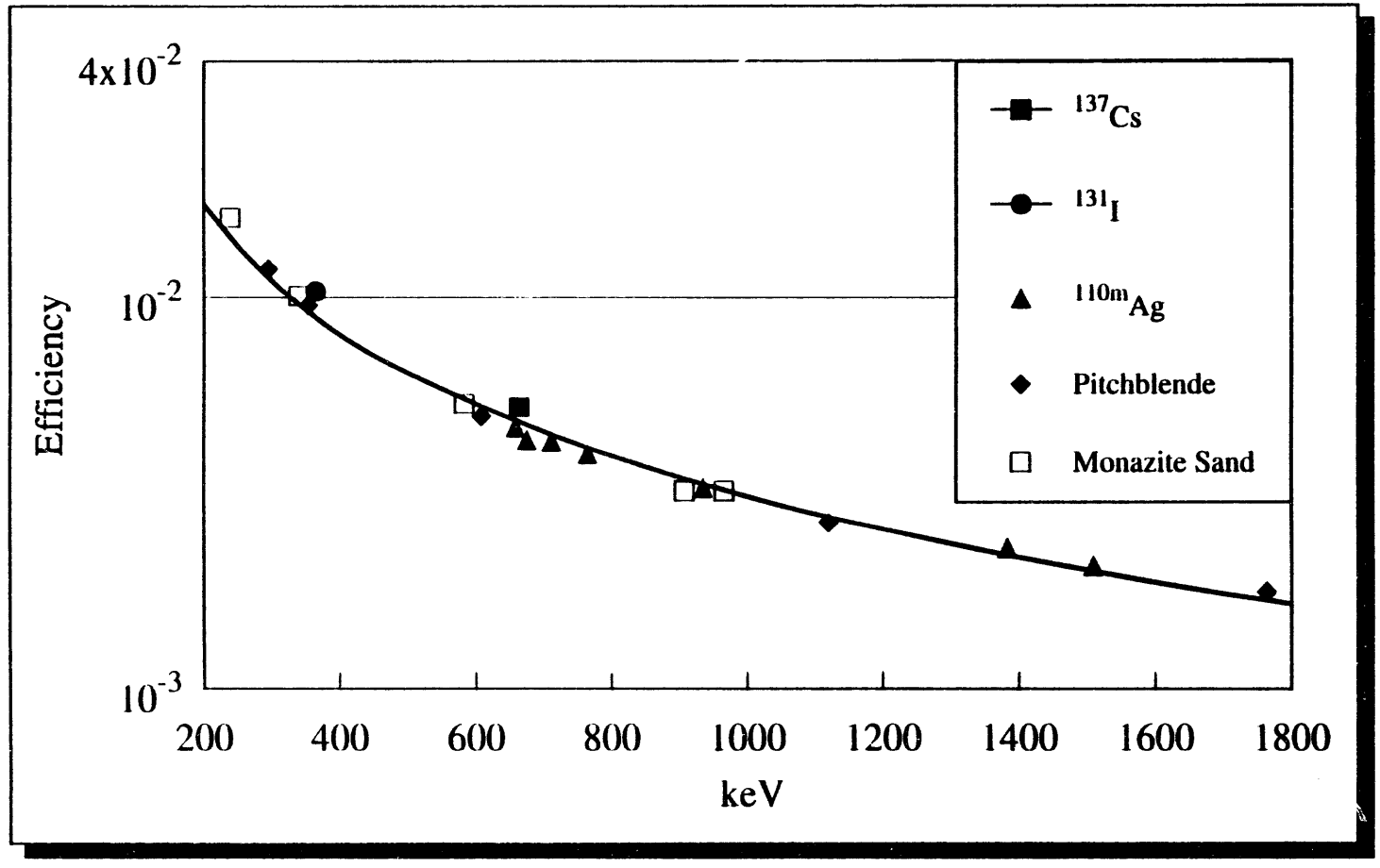

Figure 3

Self-Absorption Coefficients, Horizontal Detectors

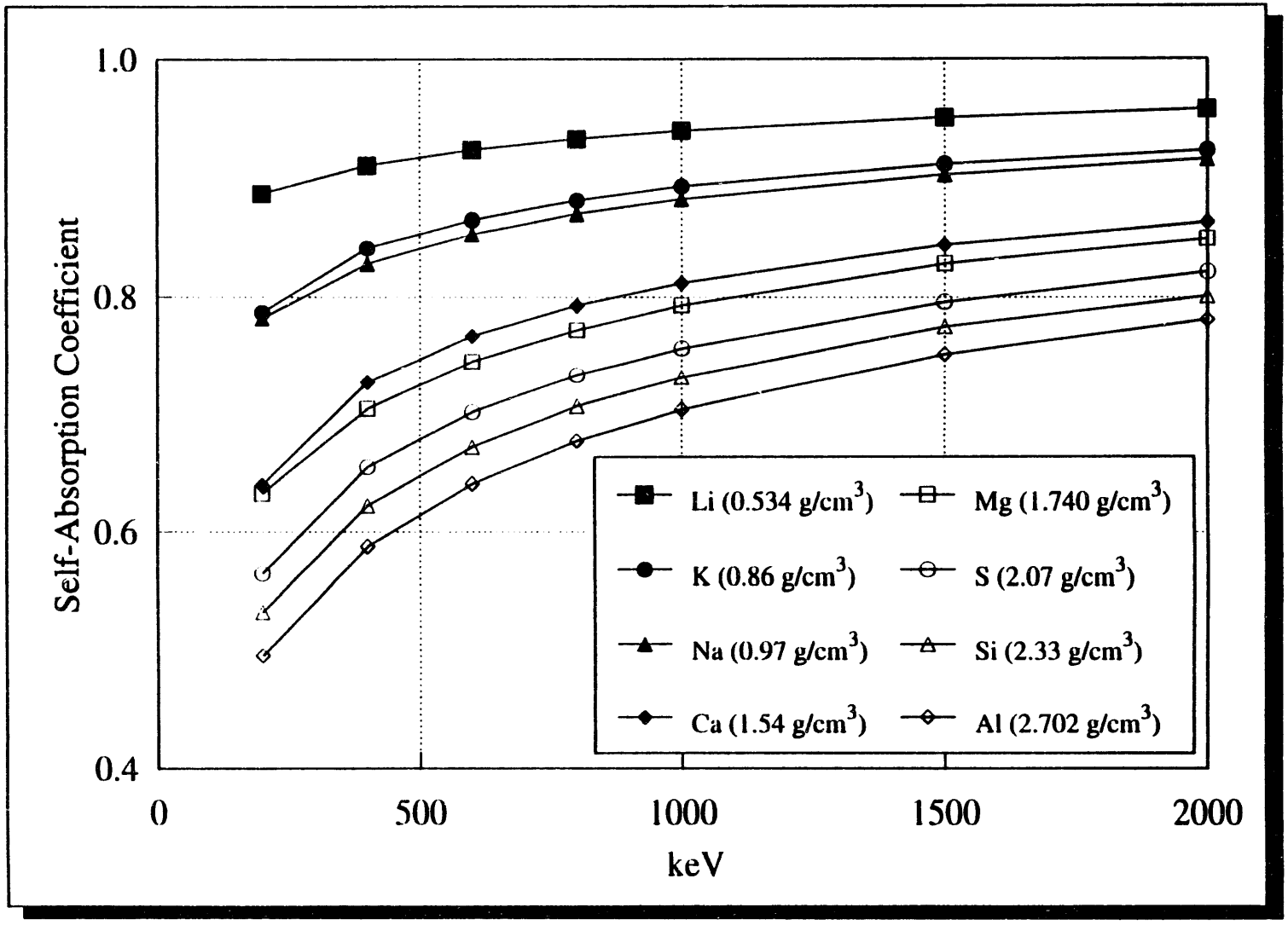

Figure 4

Correction Factors, Horizontal Detectors

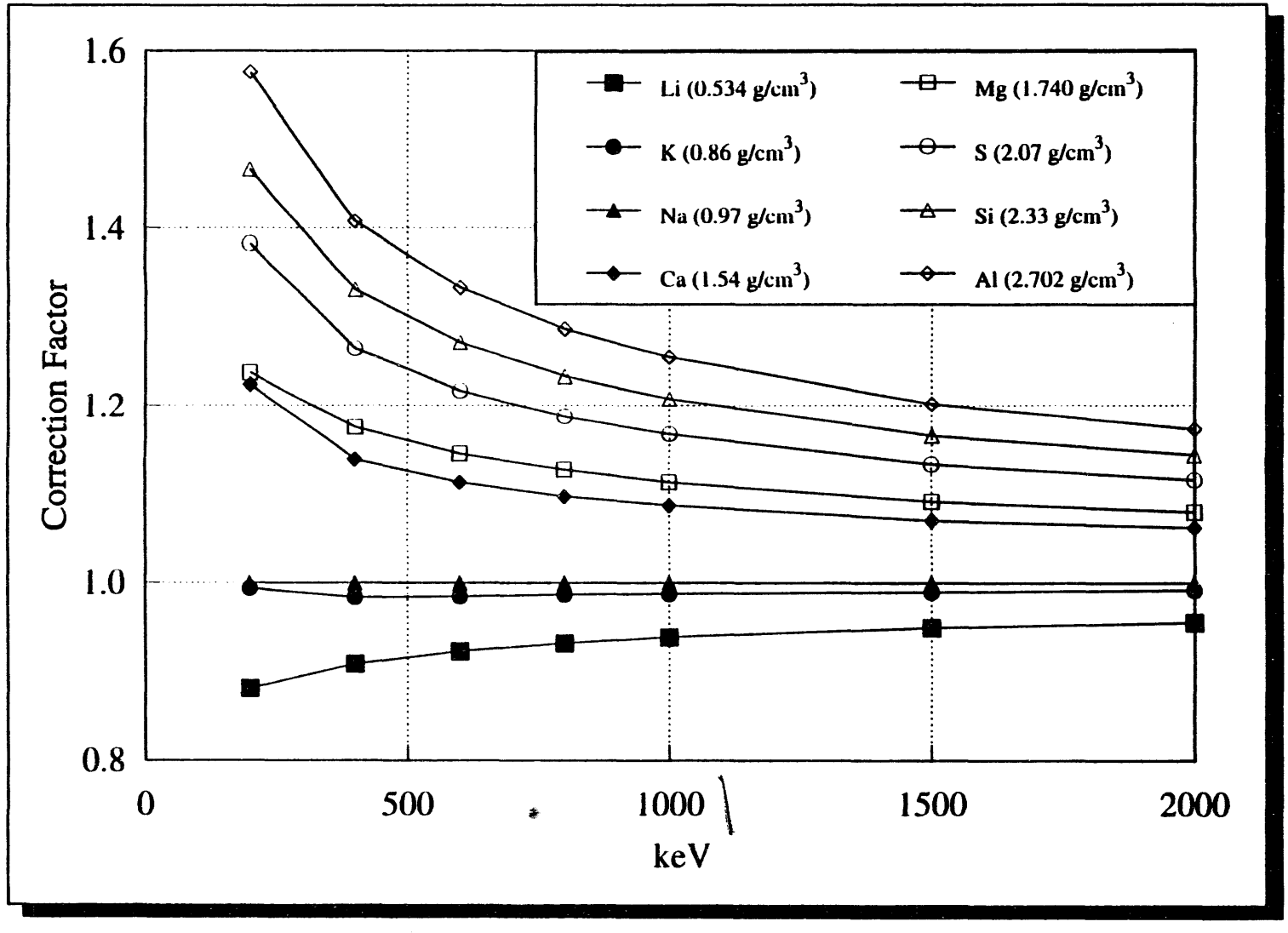

Figure 5
Horizontal Detectors

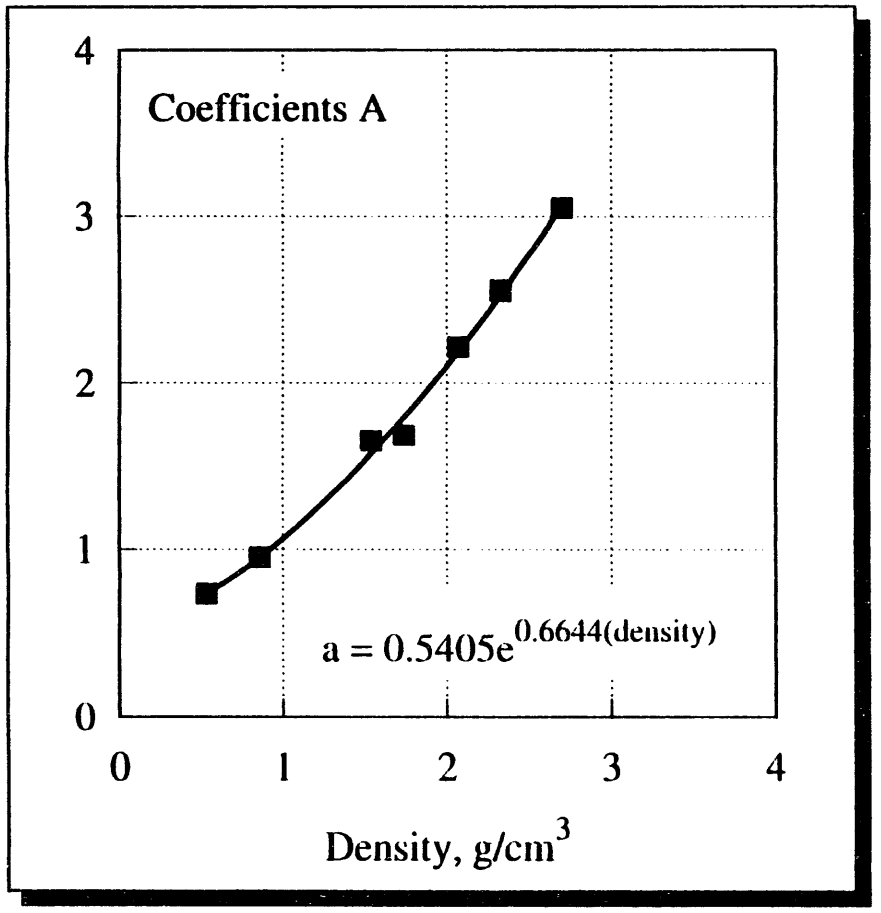

Figure 6
Horizontal Detectors

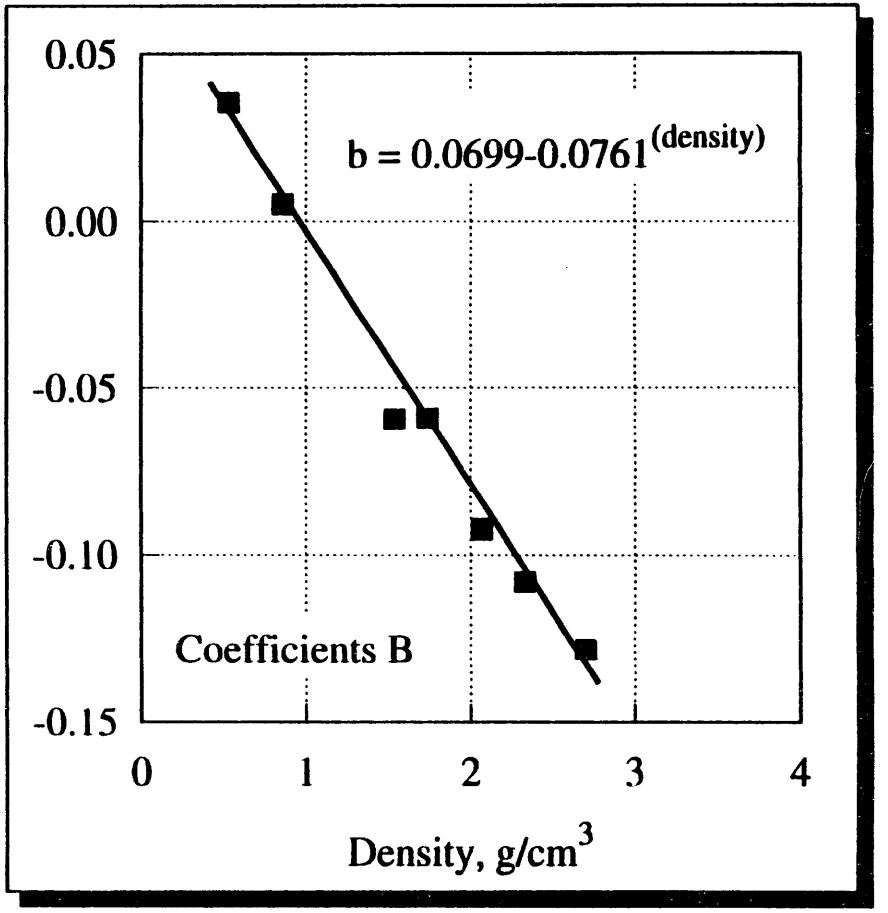

Figure 7

Soil ^{137}Cs

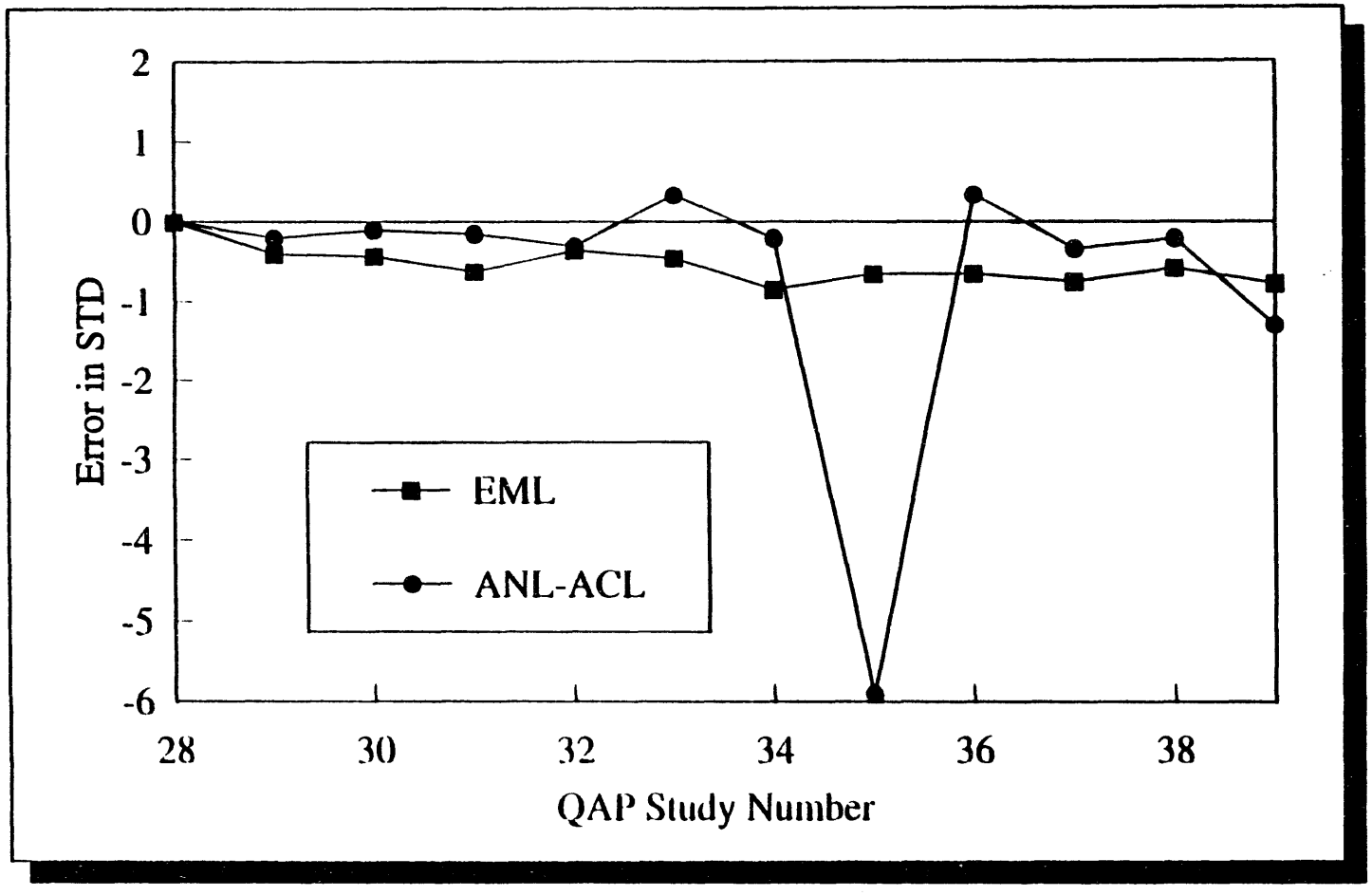

Figure 8

Vegetation ^{137}Cs

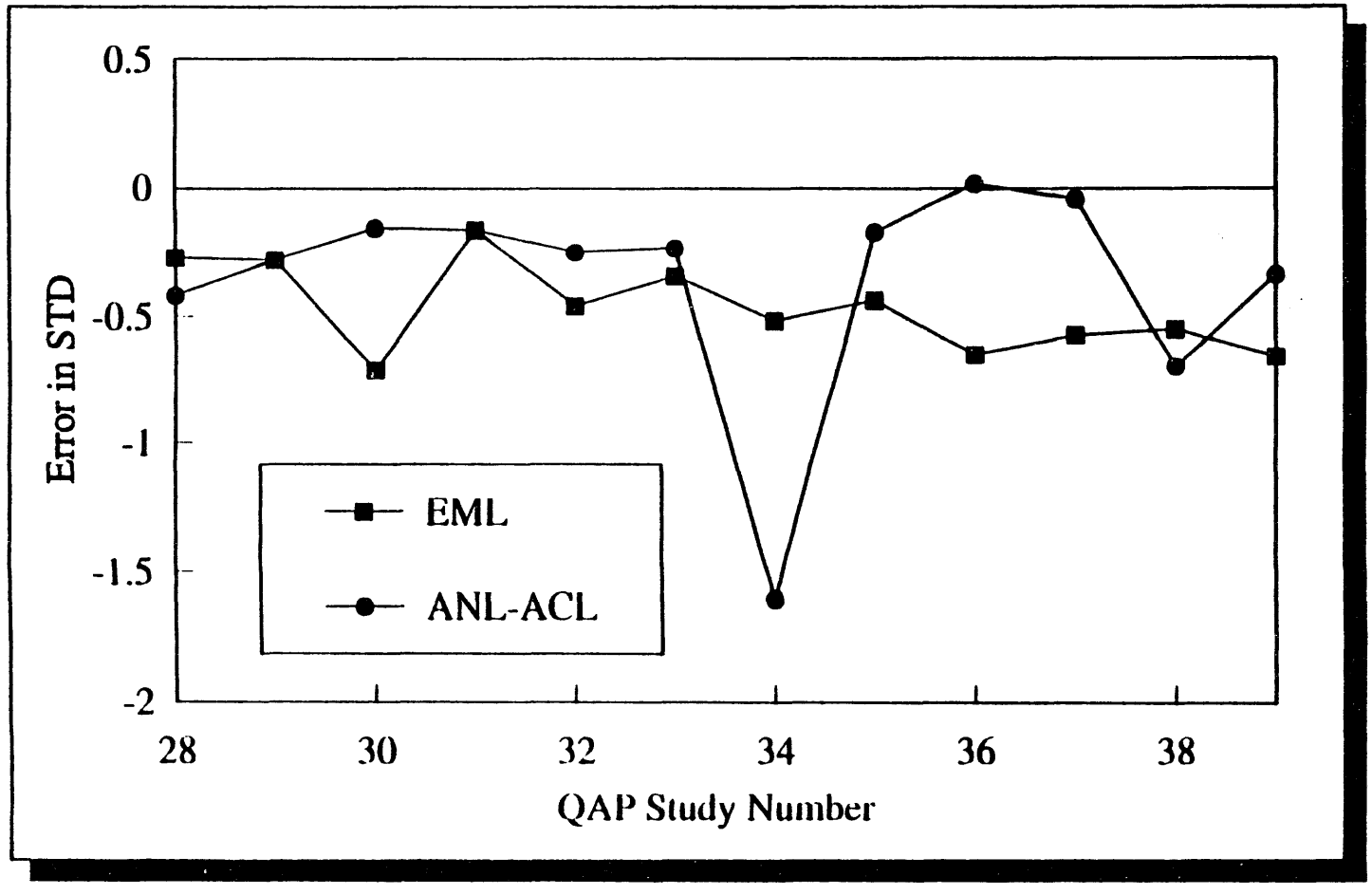

Figure 9

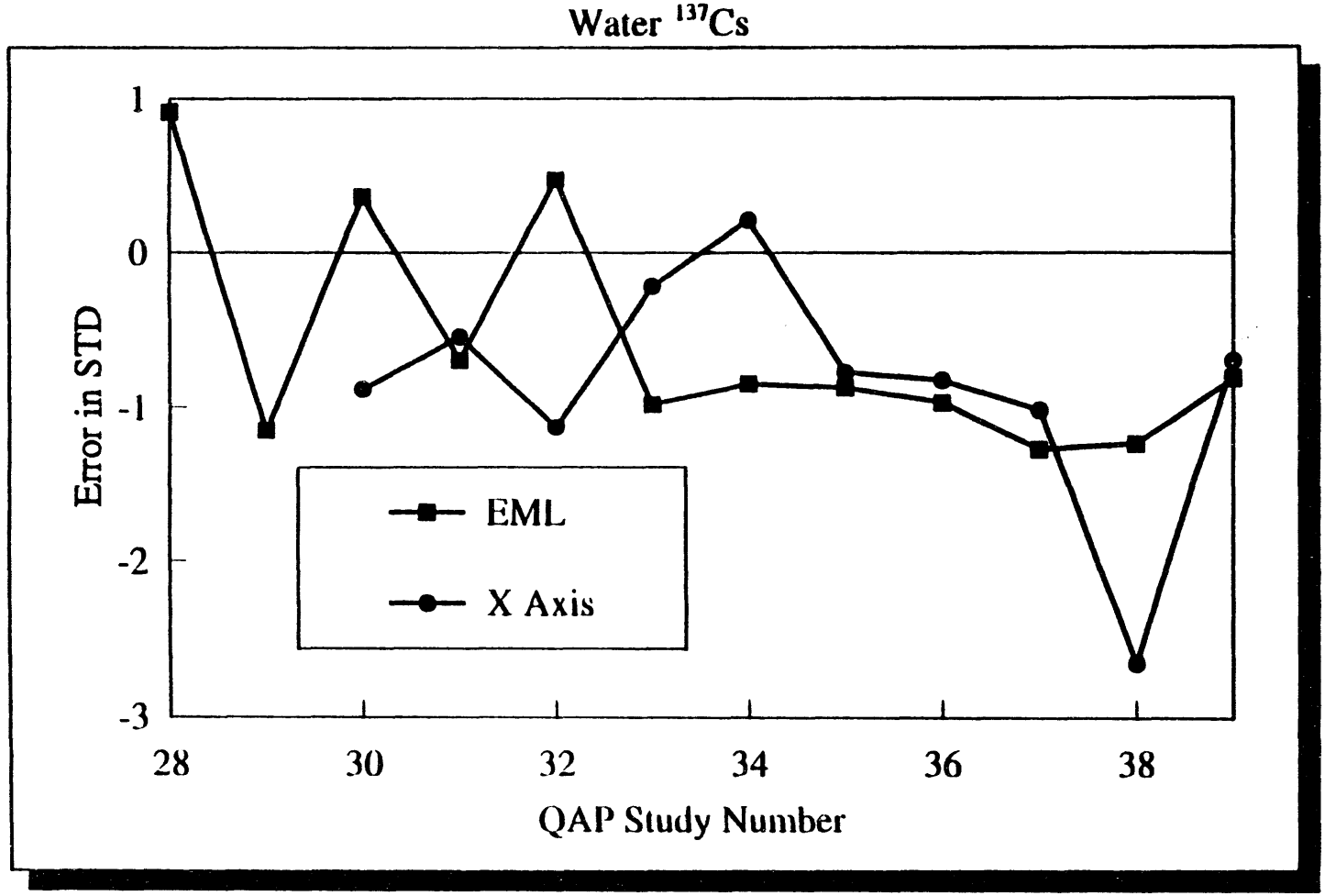
Water ^{137}Cs
Error in STD
1
0
-1
-2
-3
28
30
32
34
36
38
QAP Study Number
EML
X Axis

Table 1
Self-Absorption Coefficients
Horizontal Detector Geometries (Cylindrical Model)

$$\frac{I}{I_0} = e^{-\frac{8\,\mu_m\,\rho r}{3\pi}} \quad [1]$$

μ_m = mass absorption coefficient, cm^2/g [2]

ρ = density, g/cm^3 [3]

r = 2.5 cm

Energy, keV/ Element	Density, ρ = g/cm^3	200		400		600		800		1000		1500		2000	
		μ_m	SAF	μ_m	SAF	μ_m	SAF	μ_m	SAF	μ_m	SAF	μ_m	SAF	μ_m	SAF
Li	0.534	0.106	0.887	0.082	0.911	0.070	0.924	0.061	0.933	0.055	0.940	0..045	0.951	0.038	0.958
K	0.86	0.131	0.787	0.095	0.841	0.079	0.865	0.069	0.881	0.062	0.893	0.051	0.912	0.044	0.923
Na	0.97	0.120	0.782	0.092	0.828	0.077	0.853	0.068	0.870	0.061	0.882	0.050	0.903	0.043	0.916
Ca	1.54	0.137	0.639	0.098	0.727	0.081	0.767	0.071	0.793	0.064	0.812	0.052	0.844	0.045	0.863
Mg	1.740	0.124	0.632	0.095	0.704	0.080	0.745	0.070	0.772	0.063	0.793	0.051	0.828	0.044	0.849
S	2.07	0.130	0.565	0.097	0.654	0.081	0.701	0.071	0.733	0.064	0.756	0.052	0.796	0.045	0.821
Si	2.33	0.127	0.533	0.096	0.622	0.081	0.671	0.071	0.706	0.063	0.731	0.052	0.775	0.045	0.801
Al	2.702	0.122	0.496	0.093	0.588	0.078	0.640	0.068	0.676	0.061	0.703	0.050	0.751	0.043	0.781

Table 2
Correction Factors
Horizontal Detector Geometry
(Cylindrical Model)

$$\text{Correction Factor}_{(E)} = \frac{SAC_{(E)}\ (Na, \rho = 0.97)}{SAC_{(E)}\ (x, \rho = p_x)}$$

Element (x)	Density ρ = g/cm³	Energy, keV						
		200	400	600	800	1000	1500	2000
Li	0.534	0.881	0.909	0.923	0.932	0.939	0.950	0.956
K	0.86	0.994	0.984	0.985	0.987	0.988	0.990	0.992
Na	0.97	1.00	1.00	1.00	1.00	1.00	1.00	1.00
Ca	1.54	1.224	1.139	1.113	1.097	1.087	1.070	1.062
Mg	1.740	1.237	1.175	1.145	1.127	1.113	1.091	1.079
S	2.07	1.383	1.265	1.217	1.187	1.167	1.133	1.115
Si	2.33	1.467	1.331	1.272	1.233	1.208	1.165	1.143
Al	2.702	1.576	1.408	1.333	1.287	1.255	1.202	1.172

Table 3

Results of Curve Fitting of Horizontal Correction Factors Versus Energy

Exponential Fit: $Y = Ae^{B(X)}$ X = Energy, keV

Logarithmic Fit: $Y = A + B \ln(X)$ Y = Horizontal Correction Factor

Power Fit: $Y = A(X)^B$

Correlation Coefficients				Coefficients of Power Fit		Rel. % of Worst Fit
Density g/cm³	Exponential	Logarithmic	Power	A	B	
0.534	0.808	0.989	0.986	0.733543	0.035442	0.5
0.86	0.790*	0.984*	0.984*	0.953801	0.005118	1.4*
1.54	0.698	0.925	0.935	1.647085	-0.059530	1.9
1.740	0.814	0.983	0.988	1.681143	-0.059256	0.8
2.07	0.784	0.966	0.977	2.220774	-0.092431	1.6
2.33	0.804	0.974	0.985	2.561154	-0.107996	1.5
2.702	0.813	0.975	0.987	3.053627	-0.127890	1.6

*Without data point at 200 keV.

Table 4
Horizontal Detector Geometry (Cylindrical Model)
Comparison of Experimental Correction Factors Versus Derived Ones

Correction Factor = A (E, keV)^{B}
A = 0.540383 $e^{(0.664427 \times \text{density})}$
B = 0.069929 - 0.076091 (density)

ρ, g/cm^3	A	B	Energy, keV						
			200	400	600	800	1000	1500	2000
0.534 (E)	0.733543	0.035442	0.881	0.909	0.923	0.932	0.939	0.950	0.956
0.534 (D)	0.770533	0.029296	0.900	0.918	0.929	0.937	0.943	0.955	0.963
Rel. % Dev.	+5.0	-21.0	+2.1	+1.0	+0.7	+0.6	+0.5	+0.5	+0.7
0.86 (E)	0.953801	0.005118	0.994	0.984	0.985	0.987	0.988	0.990	0.992
0.86 (D)	0.956887	0.004491	0.980	0.983	0.985	0.986	0.987	0.989	0.990
Rel. % Dev.	+0.3	-14.0	-1.4	-0.1	-0.02	-0.10	-0.10	-0.11	-0.19
1.54 (E)	1.647085	-0.059530	1.224	1.139	1.113	1.097	1.087	1.070	1.062
1.54 (D)	1.503417	-0.047251	1.170	1.133	1.111	1.096	1.085	1.064	1.050
Rel. % Dev.	-9.6	-26.0	-4.6	-0.6	-0.2	-0.07	-0.02	-0.5	-1.2
1.74 (E)	1.681143	-0.059256	1.237	1.175	1.145	1.127	1.113	1.091	1.079
1.74 (D)	1.717081	-0.062469	1.233	1.181	1.151	1.131	1.115	1.087	1.068
Rel. % Dev.	+2.1	+5.4	-0.3	+0.5	+0.6	+0.3	+0.2	-0.3	-1.0
2.07 (E)	2.220774	-0.092431	1.383	1.265	1.217	1.187	1.167	1.133	1.115
2.07 (D)	2.138034	-0.087579	1.344	1.265	1.221	1.191	1.168	1.127	1.099
Rel. % Dev.	-3.9	-5.5	-2.9	+0.01	+0.3	+0.3	+0.05	-0.5	-1.5
2.33 (E)	2.561154	-0.107996	1.467	1.331	1.272	1.233	1.208	1.165	1.143
2.33 (D)	2.541203	-0.107363	1.439	1.336	1.279	1.239	1.210	1.159	1.124
Rel. % Dev.	-0.8	-0.6	-2.0	+0.3	+0.5	+0.6	+0.2	-0.5	-1.7
2.702 (E)	3.053627	-0.127890	1.576	1.408	1.333	1.287	1.255	1.202	1.172
2.702 (D)	3.253738	-0.135669	1.586	1.443	1.366	1.314	1.275	1.206	1.160
Rel. % Dev.	-0.8	+6.1	+0.6	+2.5	+2.5	+2.1	+1.6	+0.4	-1.7
			Predicted Correction Factors						
0.70	0.860382	-0.016665	0.940	0.951	0.957	0.962	0.965	0.972	0.977
1.25	1.239932	-0.025185	1.085	1.066	1.055	1.048	1.042	1.031	1.024

DATE
FILMED
6/30/94

END